ISSN 1674-1056
http://cpb.iphy.ac.cn
http://iopscience.iop.org/cpb
中国物理 B
Chinese Physics
中国物理
Chinese Physics B

Selection of right-circular-polarized harmonics from *p* orbital of neon atom by two-color bicircular laser fields

Chang-Long Xia(夏昌龙)[1,2], Yue-Yue Lan(兰悦跃)[1,2], Qian-Qian Li(李倩倩)[1,2], Xiang-Yang Miao(苗向阳)[1,2]
Citation: Chin. Phys. B . 2019, 28(10): 103203 . **doi:** 10.1088/1674-1056/ab4278
Journal homepage: http://cpb.iphy.ac.cn; http://iopscience.iop.org/cpb

What follows is a list of articles you may be interested in

Interpulse interference of electron emission from an atom irradiated by sinusoidally phase-modulated pulse

Hai-Ying Yuan(袁海颖), Fu-Ming Guo(郭福明), Di-Yu Zhang(张頔玉), Jun Wang(王俊), Ji-Gen Chen(陈基根), Yu-Jun Yang(杨玉军)
Chin. Phys. B . 2018, 27(10): 103201 . **doi:** 10.1088/1674-1056/27/10/103201

Simultaneous study of the lower order harmonic and photoelectron emission from an atom in intense laser pulse

Yan Yan(闫妍), Fu-Ming Guo(郭福明), Jun Wang(王俊), Ji-Gen Chen(陈基根), Yu-Jun Yang(杨玉军)
Chin. Phys. B . 2018, 27(8): 083202 . **doi:** 10.1088/1674-1056/27/8/083202

High-order harmonic generation in a two-color strong laser field with Bohmian trajectory theory

Yi-Yi Huang(黄祎祎), Xuan-Yang Lai(赖炫扬), Xiao-Jun Liu(柳晓军)
Chin. Phys. B . 2018, 27(7): 073204 . **doi:** 10.1088/1674-1056/27/7/073204

High-order harmonic generation of Li^+ with combined infrared and extreme ultraviolet fields

Li Wang(王力), Guo-Li Wang(王国利), Zhi-Hong Jiao(焦志宏), Song-Feng Zhao(赵松峰), Xiao-Xin Zhou(周效信)
Chin. Phys. B . 2018, 27(7): 073205 . **doi:** 10.1088/1674-1056/27/7/073205

Modulation of multiphoton resonant high-order harmonic spectra driven by two frequency-comb fields

Yuanyuan Zhao(赵媛媛), Di Zhao(赵迪), Chen-Wei Jiang(蒋臣威), Fu-li Li(李福利)
Chin. Phys. B . 2018, 27(5): 053202 . **doi:** 10.1088/1674-1056/27/5/053202

Selection of right-circular-polarized harmonics from p orbital of neon atom by two-color bicircular laser fields*

Chang-Long Xia(夏昌龙)[1,2], Yue-Yue Lan(兰悦跃)[1,2], Qian-Qian Li(李倩倩)[1,2], and Xiang-Yang Miao(苗向阳)[1,2,†]

[1] College of Physics and Information Engineering, Shanxi Normal University, Linfen 041004, China
[2] Key Laboratory of Spectral Measurement and Analysis of Shanxi Province, Shanxi Normal University, Linfen 041004, China

(Received 2 July 2019; revised manuscript received 5 August 2019; published online 30 September 2019)

The polarization properties of high-order harmonic generation (HHG) in the two-color circularly polarized laser fields are investigated by numerically solving the two-dimensional time-dependent Schrödinger equation. By adding a wavelength of 1600-nm right-circular-polarized field to an 800-nm left-circular-polarized field, HHG is simulated from a real model of neon atom with p orbital, but not from a hydrogen-like atom model with s orbital. The orders of $3n+1$ can be selected while the orders of $3n+2$ are suppressed by adjusting the intensities of the two pulses. The physical mechanism is analyzed by time–frequency analysis and semiclassical model.

Keywords: high-order harmonic generation, circular polarization field, polarization selection

PACS: 32.80.Rm, 42.65.Ky, 42.65.Re **DOI:** 10.1088/1674-1056/ab4278

1. Introduction

High-order harmonic generation (HHG) which is a useful tool to monitor quantum dynamics has been intensively investigated.[1–7] HHG could be used to produce attosecond pulse[8–12] that is a powerful tool to probe, track, control the dynamics of electron in ultrafast process.[13–16] Recently, linearly polarized attosecond pulse could be obtained from linear polarized harmonics in experiments,[17,18] and the HHG process is well described by semiclassical three-step model.[13] In circular or highly elliptical field, the atoms or molecules have a probability to be ionized but the electron scarcely ever recombines to the parent ion, thus circular-polarized harmonic (CPH) is hardly obtained by using a circular driver fields.[19,20] However, a CPH signal is needed to well understand the chiral-sensitive phenomena such as ultrafast chiral-specific dynamics in molecules, the character of magnetic materials and nanostructures, and so on.[21–23] So that the CPH generation[24–27] and its potential application[28] are a hot topic in very recent years.

Counter rotating bicircular (CRB) field scheme has been proposed to generate CPH or highly elliptical light pulses. Generally, this scheme combines a right-circular-polarized (RCP) pulse with a left-circular-polarized (LCP) second harmonics, first proposed in Ref. [29]. This scheme was proven experimentally[30] and it has been applied to generate an attosecond pulse recently.[31,32] For the combination field, a trefoil structure would be obtained in Lissajous curve with a threefold symmetry: the system remains constant by the combination of 120° rotation and a time delay of one-third of the fundamental frequency field period.[33] For centrally symmetric system such as atom targets, the harmonic orders of $3n+1$ and $3n+2$, which correspond to RCP and LCP harmonics respectively can be generated. The harmonic orders of $3n$ are absent because of the symmetry.[24,31,32,34–36] For the molecule targets, odd–even harmonics can also be emitted due to the asymmetry of the initial-state electron wave function,[37,38] hence the selection rules are more elaborate because it based on both the symmetry of the target and the symmetry of the field.[39–42] A linearly attosecond pulse can be obtained when the intensities of RCP and LCP harmonics are equal. Consequently, it would be meaningful if the high elliptically or circularly attosecond pulse can be obtained which means the ellipticity of the attosecond pulse can be controlled.

CPH generation is investigated from rare gas, such as helium, neon, argon, both in experiments and in theory. As we all know, the ground state of those gases is p orbital except helium and has three degenerate orbitals sign as p_+ $(m=1)$, p_- $(m=-1)$, p_0 $(m=0)$. In this paper, the HHG from the p orbital of neon atom by the CRB field is theoretically investigated. Since the Ne atoms with closed electron shells, a hydrogen-like model to simulate Ne atoms can also satisfy the selection rules as the p orbital:[43] $N\omega=(3n\pm1)\omega$ (n is an integer). But it cannot simulate the intensity regularities between adjacent harmonics well.[24,43] Our work intends to focus on the selection of the same helicity, thus choosing the p orbital as the initial state is necessary. The helicity of HHG is studied by calculating the phase differences between x and y components. The right-circular-polarized harmonics could be

*Project supported by the National Natural Science Foundation of China (Grant Nos. 11974229, 11504221, and 11404204), the Scientific and Technological Innovation Program of Higher Education Institutions in Shanxi Province, China (Grant No. 2019L0452), the Natural Science Foundation for Young Scientists of Shanxi Province, China (Grant No. 2015021023), and the Program for Top Young Academic Leaders of Higher Learning Institutions of Shanxi Province, China.

†Corresponding author. E-mail: sxxymiao@126.com

© 2019 Chinese Physical Society and IOP Publishing Ltd

selected in the p orbital of the neon atom by adjust the relative intensity of the pulses. Time–frequency analysis and the semi-classical three-step model are used to study the short and long paths.

2. Theory and method

We numerically calculate the HHG by solving the time-dependent Schrödinger equation (TDSE). The TDSE can be expressed as (in atomic units)

$$\mathrm{i}\frac{\partial \Psi(x,y,t)}{\partial t} = \left[-\frac{\nabla^2}{2} + V(x,y) + x\cdot E_x(t) + y\cdot E_y(t)\right]\Psi(x,y,t). \quad (1)$$

$V(x,y)$ is the two-dimensional potential and for the neon atom can be written as[23,44]

$$V(x,y) = -\frac{1+9\,\mathrm{e}^{-(x^2+y^2)}}{\sqrt{x^2+y^2+a}}, \quad (2)$$

where $a = 2.882$ to simulate the $2p$ orbital of the neon atom. The combination field of CRB scheme is

$$\boldsymbol{E}(t) = \frac{E_0 f(t)}{\sqrt{1+\gamma^2}}(\cos(\omega_1 t) + \gamma\cos(\omega_2 t))e_x + \frac{E_0 f(t)}{\sqrt{1+\gamma^2}}(\sin(\omega_1 t) - \gamma\sin(\omega_2 t))e_y, \quad (3)$$

where ω_1 field is the RCP and ω_2 is the LCP. γ is the electric field ratio of LCP pulse to RCP pulse. $f(t)$ is the laser envelope with a flat top and two ramps described by the $\sin^2$ function:

$$f(t) = \begin{cases} \sin^2\left(\dfrac{\pi t}{4T}\right), & 0 \le t \le 2T, \\ 1, & 2T \le t \le 6T, \\ \sin^2\left(\dfrac{\pi(t-8T)}{4T}\right), & 6T \le t \le 8T, \end{cases} \quad (4)$$

where $T = 2\pi/\omega_1$. This type of envelope has been proved to get more perfect circular polarization of high-order harmonics than others.[6] From Ehrenfest theorem, the dipole accelerations in two components are given by

$$a_x(t) = \left\langle \Psi(x,y,t)\left| -\frac{\partial V(x,y)}{\partial x} - E_x(t)\right|\Psi(x,y,t)\right\rangle, \quad (5)$$

$$a_y(t) = \left\langle \Psi(x,y,t)\left| -\frac{\partial V(x,y)}{\partial y} - E_y(t)\right|\Psi(x,y,t)\right\rangle. \quad (6)$$

The power of the harmonic spectra in two components are proportional to

$$S_x(\omega) \sim |a_x(\omega)|^2 = \left|\int a_x(t)\,\mathrm{e}^{-\mathrm{i}\omega t}\,\mathrm{d}t\right|^2, \quad (7)$$

$$S_y(\omega) \sim |a_y(\omega)|^2 = \left|\int a_y(t)\,\mathrm{e}^{-\mathrm{i}\omega t}\,\mathrm{d}t\right|^2. \quad (8)$$

And the total power is obtained by

$$S_{\mathrm{total}}(\omega) = S_x(\omega) + S_y(\omega). \quad (9)$$

The relative harmonic phase differences between the polarized components of the emitted harmonics can be obtained as

$$\delta(\omega) = \arg[a_x(\omega)] - \arg[a_y(\omega)]. \quad (10)$$

If $S_x(\omega) = S_y(\omega)$ and $\delta(\omega) = \pm\pi/2$, the harmonic is strictly circular-polarized.

3. Results and discussion

To simulate the HHG from $2p$ orbital of neon, we numerically solve Eq. (1) with the initial state in two cases by the method used in Ref. [24]. The initial states for $m = \pm 1$ are defined as $p_\pm = p_x \pm \mathrm{i}p_y$, the p_0 orbital is neglected because it has a node in the polarization plane and the contribution to the HHG is too weak from the p_0 orbital.[40] In our simulation, the CRB field is combined by a $\lambda_1 = 1600$-nm RCP pulse with $\lambda_2 = 800$-nm LCP pulse, and the intensity of each field is $I_1 = I_2 = 0.5\times10^{14}$ W/cm^2. First, we investigate HHG for the initial state in p_+ orbital, as shown in the left column of Fig. 1. To clearly show the harmonic orders in the plateau area, figure 1(a) shows the harmonic spectra from 30th order to 90th order. The overall character of the HHG is shown in the inset of Fig. 1(a). The following characters are obviously observed from harmonic spectra: (i) The harmonic orders of $3n+1$ and $3n+2$ are obtained in the whole plateau area and the intensities of $3n+2$ orders are lower than the $3n+1$ orders. (ii) The intensity of the spectrum in x component is approximately equal to the intensity in y component at each $3n+1$ order. We also calculate the phase difference of the HHG by Eq. (10), and the result is shown in Fig. 1(c), the orders of $3n+1$ and $3n+2$ are marked by the red solid circle and the blue solid square, respectively. The phase differences are stable near $\pi/2$ for harmonic orders of $3n+1$ while fluctuant near the $-\pi/2$ for the orders of $3n+2$. Because the harmonic intensities are equal at the x and y components and the phase differences are nearly $\pi/2$, the harmonic orders of $3n+1$ correspond to perfect RCP harmonic.

Second, we investigate HHG for the initial state in p_- orbital, as shown in the right column of Fig. 1. Contrary to the situation of p_+: (I) The intensities of $3n+2$ orders are higher than the $3n+1$ orders. (II) The harmonic intensities between the x and y components are almost equal at each $3n+2$ order. (III) The phase differences are stable near $-\pi/2$ for harmonic orders of $3n+2$ while fluctuant near the $\pi/2$ for the orders of $3n+1$. Based on the above phenomenon and analyses, perfect LCP harmonic could be obtained at the orders of $3n+2$ in p_- orbitals. From Figs. 1(b) and 1(d), the phase differences are not stable for the $3n+2$ or $3n+1$ orders, thus left-handed or right-handed elliptically polarized harmonics can be obtained in p_+, p_- orbitals. However, the real initial state of neon atom is coupled by p_+ and p_- orbitals, it is necessary to calculate the total harmonic spectrum to simulate the phenomenon in the experiment.

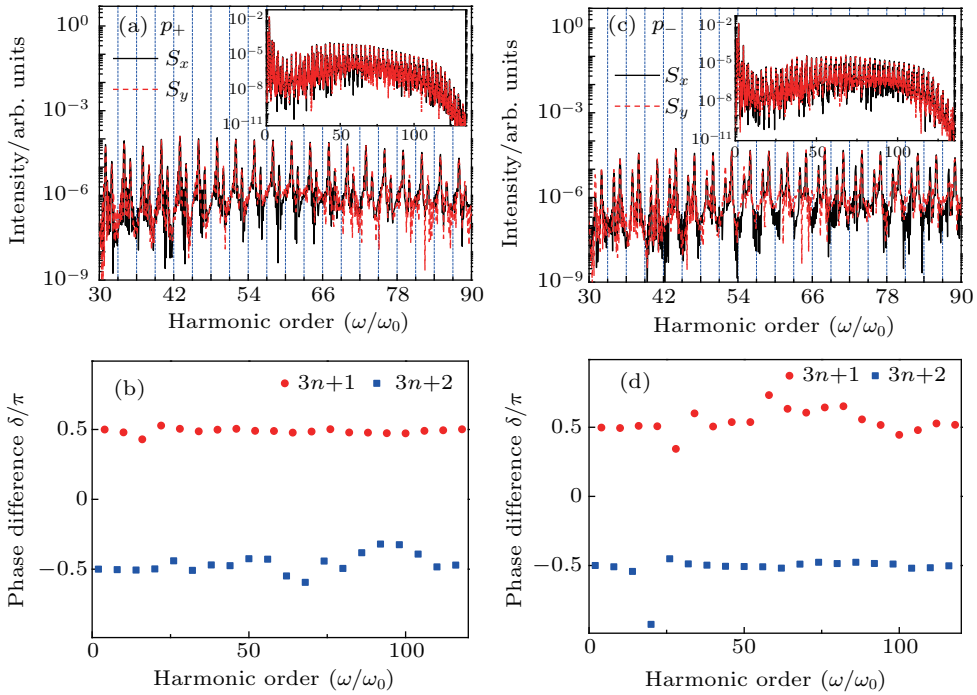


Fig. 1. Harmonic spectra from the initial state p_+ (left column) and p_- (right column) states. The red solid line and the blue dashed line represent the x component and the y component, respectively. (a) and (c) 30th–90th orders. The insets show the overlook of the whole harmonic spectra structure. (b) and (d) The phase differences between x and y components. The red solid circles and the blue solid squares represent $3n+1$ and $3n+2$ orders, respectively. The parameters of the two laser pulses are $\lambda_1 = 2\lambda_2 = 1600$ nm and $I_1 = I_2 = 0.5 \times 10^{14}$ W/cm^2.

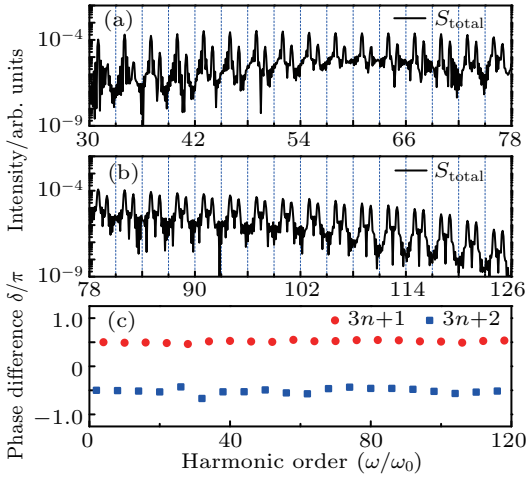


Fig. 2. The total spectra obtained by adding the contributions from the p_+ orbital and p_- orbital coherently. (a) 30th–78th orders, (b) 78th–126th orders. (c) The phase differences between x and y components. The red circles and the blue squares represent $3n+1$ and $3n+2$ orders, respectively. The laser parameters are the same as those in Fig. 1.

The total spectra of HHG are calculated by Eqs. (7)–(9), and the total dipole acceleration in x (y) component is obtained by $a_i^{\text{total}}(t) = a_i^{p+}(t) + a_i^{p-}(t)$ (i is x or y). Figures 2(a) and 2(b) show the total HHG, the orders of $3n+1$ and $3n+2$ appear in the whole plateau region. The intensities of $3n+1$ orders are higher than $3n+2$ orders, the electron in continuum state is affected more strongly by the lower-frequency field, thus the polarization of the harmonics is affected more strongly by the fundamental field, that is the RCP. From Fig. 2(c), the phase differences in the plateau region are stable at $\pi/2$ and $-\pi/2$ for the harmonic orders of $3n+1$ and $3n+2$, *i.e.*, a pair of perfect circular-polarized harmonics with RCP and LCP are obtained, respectively. As mentioned in Ref. [19], linearly attosecond pulses will be synthesized if RCP and LCP harmonics have the same intensities. Therefore, while keeping RCP and LCP harmonics in perfect circular-polarization, RCP or LCP could be selected and a simple and straightforward method to generate highly elliptically or circularly attosecond pulse trains is desirable.

The mechanism of HHG is further discussed by the time-frequency analysis in synchro squeezing transforms (SST) method. The SST can solve the problem of spectrum ambiguity and analyze lower orders harmonic more clearly.[45,46] Figure 3(a) shows the time–frequency analysis by transforming the total dipole acceleration in x component. Three quantum paths are obtained in each optical cycle. The HHG is mainly contributed by short paths which are marked by A_x, B_x, and C_x in the optical cycle of $[2.8T_1, 3.8T_1]$. The intensity of A_x is stronger than those of B_x and C_x in the above-threshold region (above 28th order). In the below-threshold region, the intensities of the three peaks are weak, corresponding to the weak spectra in this region as shown in the inset of Fig. 1. For the case of y component, the time–frequency analysis is shown in Fig. 3(b). There are also three quantum paths in each optical cycle. However, the intensity of A_y is very weak and the intensity of B_y is stronger than the peak of C_y in the region of above threshold. Why are the intensities of three peaks different on x component and y component? We will discuss the reason by the semiclassical three-step model.

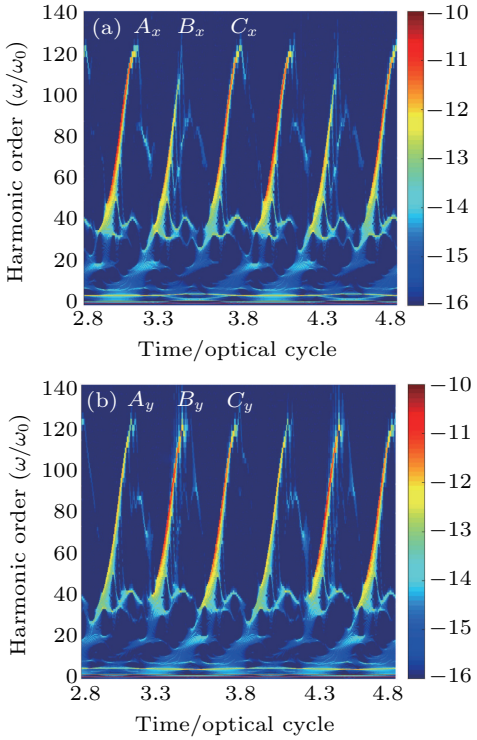


Fig. 3. The SST time–frequency analysis by transforming the total dipole acceleration in two components. Panels (a) and (b) show the x and y components, respectively. The laser parameters are taken to be the same as those in Fig. 2.

As everyone knows, the field is threefold symmetry in one cycle for the case of $\omega_2 = 2\omega_1$. The combined CRB field is shown in Fig. 4(a), the inset is Lissajous curves of the combination field in plateau region of the trapezoidal envelope, the lobes A, B, C are marked with background colors of gray, red, and green in one-cycle electric field of the pulse. The threefold symmetry leads to the three paths[35,47] as discussed in Fig. 3. To give a clear picture of the HHG, we solve the Newton's equation under the CRB field.[48–50] The initial velocity in x component (*i.e.*, OA direction) is set to zero but the initial velocity in y component is nonzero when the ionization time is in lobe A, as discussed in Ref. [44]. For the case of ionization time in lobe B or lobe C, we set the initial velocity to zero at the OB or OC direction, and set to non-zero at the direction perpendicular to OB or OC, the similar results can be obtained due to the symmetry of the threefold. Figure 4(b) shows kinetic energy in unit of $\hbar\omega_1$, two kinetic energy peaks which ionized in lobe C are marked with P_{i1} and P'_{i1}, and the corresponding emission times in lobe A and lobe B are marked with P_{e1} and P'_{e1} respectively. Although short and long paths are obtained from classical model, HHG is mainly contributed by short path in fact,[35,44] and this character can also be found from Fig. 3. The intensities of HHG contributed from long path may lower due to the wave function diffusion in the laser field. So in order to understand characteristics of HHG more clearly, short path is mainly studied. Moreover, the time of electron oscillation is longer for the peak P'_{e1} than P_{e1}, thus the electron mainly recombines to the parent nucleus in peak P_{e1} for the case ionized from lobe C. Similarly, for the ionization time in the region of lobe A or lobe B, HHG are mainly contributed by the peaks P_{e2} and P_{e3}. Those three peaks are corresponding to the quantum paths $A_{x(y)}$, $B_{x(y)}$, and $C_{x(y)}$, respectively.

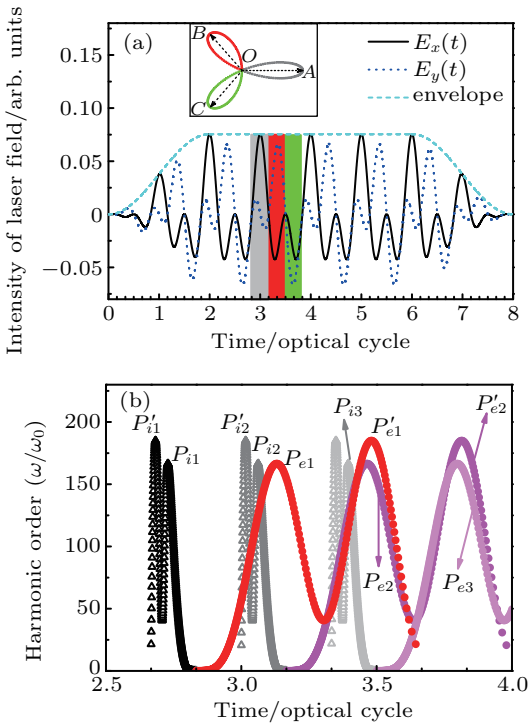


Fig. 4. (a) The combined laser field with an envelope shape. The solid black line, blue dotted line, and cyan dashed line represent the x, y components and the envelope shape. The colors of background are painted in gray, red, and green, corresponding to lobes A, B, and C as shown in Lissajous curve of the inset. (b) The kinetic energy obtained from semiclassical three-step model. Black, gray, and light gray triangles represent the ionization times at lobes C, A, and B, the corresponding emission times are represented by red, magenta, and pink circles, respectively.

The emission time of short quantum path is analyzed to explain the relative intensity of the quantum paths. In the time range of peak P_{e1}, $|E_x| > |E_y|$, which is corresponding to time range marked by gray background in Fig. 4(a). So that the electron recombines to the parent nucleus in x component is stronger, this maybe the reason the intensity of quantum path A_x is much larger than that of the path A_y. The phenomenon could also be verified for the paths $B_{x(y)}$ and $C_{x(y)}$. In the time range of peaks P_{e2} and P_{e3}, the electric field strength in x component is weaker than that in y component, thus the intensities of B_x and C_x are weaker than those of B_y and C_y. The semiclassical three-step model gives a clear physical picture, which qualitatively explains physical process and relative intensity of the quantum paths.

In order to select right-circular-polarized harmonics, we keep the total intensities of RCP and LCP pulses unchanged and try to adjust the intensity ratio I_2/I_1 by changing the amplitude ratio γ. Figure 5(a) shows harmonic spectra when $\gamma = 0.8$, compared with Fig. 2(a), we find that the intensities of harmonics are slightly decreased in the whole plateau region,

and the intensities of $3n+2$ orders get weaker. To clearly analyze the relation of the intesity, we define a quantitative parameter χ to show relative intensity between $3n+1$ and $3n+2$ orders of the harmonic:

$$\chi(n) = \frac{S(3n+1) - S(3n-1)}{S(3n+1) + S(3n-1)},$$

where $S(i)$ is the intensity of the i-th order, $i = 3n+1$ or $3n+2$. From Fig. 5(c), contrasting the $\gamma = 1$ and $\gamma = 0.8$ for the p orbital, we note that the relative intensity χ is greater than 0.64, which means the intensities of $3n+1$ orders are stronger than those of $3n+2$ orders in both cases. The relative intensity for the case of $\gamma = 0.8$ is higher than $\gamma = 1$ obviously. Even the value of χ is close to 1 when $n = 11$, 13, indicating that the $3n+2$ orders harmonics are almost suppressed. We also try other values of γ (not shown here) and find the harmonics of the same helicility as the fundamental field could be selected by changing the intensity ratio, but the intensities of the overall harmonic will decrease as the intensity ratio decreases.

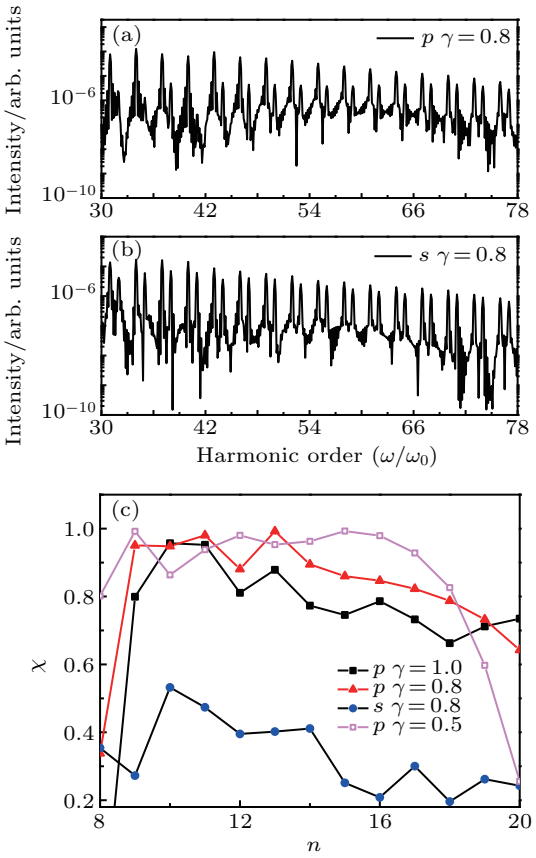


Fig. 5. (a) and (b) Harmonic spectra generated from p orbital and s orbital for the case of $\gamma = 0.8$. (c) The relative intensity for p and s orbitals. The black solid square, red solid triangle, and pink hollow square represent $\gamma = 1$, $\gamma = 0.8$, and $\gamma = 0.5$ for p orbital, respectively. The blue circle represents $\gamma = 0.8$ for s orbital. The other laser parameters are keeping the same as those in Fig. 2.

Could the intensity ratio affect the harmonic generation from hydrogen-like model of the neon atom in three fold electric field? The hydrogen-like model whose potential is taken from $V(r) = -1/\sqrt{r^2 + 0.1195}$ is used to simulate the neon atom. The harmonic spectra of the neon atom with s orbital as the initial state under the same laser pulses irradiation is shown in Fig. 5(b). The intensities of $3n+1$ orders harmonics are a little stronger than those of $3n+2$ orders for the case of $\gamma = 0.8$, and they are decreased in pair after 70th order. As shown in Fig. 5(c), the relative intensity $\chi(n)$ of harmonics is less than 0.54. By analyzing s orbital, the right-circular-polarized harmonics can also be selected by changing the intensity ratio, while the effect of enhancing is really weak. From the above discussion, we can achieve the selection of right-circular-polarized harmonics by laser field action on the p orbital of the neon atom with increasing the intensities of RCP pulse. We atrribute the selection of the right-circular-polarized harmonics to the stronger effect of the fundamental field, which leads to probability of recombination on p_+. So when the intensities of RCP pulse are increased, the intensities of harmonic whose helicity direction is the same as RCP pulse could be enhanced.

4. Conclusion

In summary, we theoretically investigated HHG from a $2p$ orbital neon atom in intense CRB field. A pair of circular-polarized harmonics with RCP and LCP are obtained at the orders of $3n+1$ and $3n+2$, which is corresponding to the results in experiments. Time–frequency analysis shows that three short quantum paths $A_{x(y)}$, $B_{(x(y))}$, and $C_{(x(y))}$ contributing to HHG in each optical cycle, and their intensities are different between x component and y component. The classical three-step model is used to reconstruct the three quantum paths and explain the reason why the intensities are different. It is found that the right-circular-polarized harmonics can be selected in the p orbital of the neon atom by changing the intensity ratio. Our research establishes a good correspondence between the quantum path and the classical trajectory, which provides a valuable scheme on generating highly elliptically or circularly attosecond pulse trains.

References

[1] Baker S, Robinson J S, Haworth C A, Teng H, Smith R A, Chirilă C C, Lein M, Tisch J W G and Marangos J P 2006 *Science* **312** 424
[2] Wörner H J, Bertrand J B, Kartashov D V, Corkum P B and Villeneuve D M 2010 *Nature* **466** 604
[3] Xia C L, Zhang J, Miao X Y and Liu X S 2017 *Chin. Phys. B* **26** 073201
[4] Zhang C P, Xia C L, Jia X F and Miao X Y 2017 *Sci. Rep.* **7** 10359
[5] Wu H, Yue S, Li J, Fu S, Hu B and Du H 2018 *Chin. Opt. Lett.* **16** 040203
[6] Heslar J, Telnov D A and Chu S I 2019 *Phys. Rev. A* **99** 023419
[7] Shao J, Zhang C P, Jia J C, Ma J L and Miao X Y 2019 *Chin. Phys. Lett.* **36** 054203
[8] Wu J S, Jia Z M and Zeng Z N 2017 *Chin. Phys. B* **26** 093201
[9] Zhong H Y, Guo J, Zhang H D, Du H and Liu X S 2015 *Chin. Phys. B* **24** 073202
[10] Du H, Luo L, Wang X and Hu B 2012 *Opt. Express* **20** 9713
[11] Xia C L, Liu Q Y and Miao X Y 2018 *Opt. Commun.* **407** 127
[12] Xia C L and Liu X S 2013 *Phys. Rev. A* **87** 043406
[13] Corkum P B 1993 *Phys. Rev. Lett.* **71** 13

[14] Kelkensberg F, SiuW, Pérez-Torres J F, Morales F, Gademann G, Rouzée A, Johnsson P, Lucchini M, Calegari F, Sanz-Vicario J L, Martín F and Vrakking M J J 2011 *Phys. Rev. Lett.* **107** 043002

[15] Garg M, Zhan M, Luu T T, Lakhotia H, Klostermann T, Guggenmos A and Goulielmakis E 2016 *Nature* **538** 359

[16] He L, Zhang Q, Lan P, Cao W, Zhu X, Zhai C, Wang Feng, Shi W, Li M, Bian X B, Lu P and Bandrauk A D 2018 *Nat. Commun.* **9** 1108

[17] Goulielmakis E, Schultze M, Hofstetter M, Yakovlev V S, Gagnon J, Uiberacker M, Aquila A L, Gullikson E M, Attwood D T, Kienberger R, Krausz F and Kleineberg U 2008 *Science* **320** 1614

[18] Gaumnitz T, Jain A, Pertot Y, Huppert M, Jordan I, Ardana-Lamas F and Wörner H J 2017 *Opt. Express* **25** 27506

[19] Dorney K M, Ellis J L, Hernández-García C, Hickstein D D, Mancuso C A, Brooks N, Fan T, Fan G, Zusin D, Gentry C, Grychtol P, Kapteyn H C and Murnane M M 2017 *Phys. Rev. Lett.* **119** 063201

[20] Jimeńez-Galań Á, Zhavoronkov N, Ayuso D, Morales F, Patchkovskii S, Schloz M, Pisanty E, Smirnova O and Ivanov M 2018 *Phys. Rev. A* **97** 023409

[21] Neufeld O and Cohen O 2018 *Phys. Rev. Lett.* **120** 133206

[22] Cireasa R, Boguslavskiy A E, Pons B, Wong M C H, Descamps D, Petit S, Ruf H, Thiré N, Faerré A, Higuet J, Schmidt B E, Alharbi A F, Légaré F, Blanchet V, Fabre B, Patchkovskii S, Smirnova O, Mairesse Y and Bhardwaj V R 2015 *Nat. Phys.* **11** 654

[23] Fan T, Grychtol P, Knut R, *et al.* 2015 *PNAS* **112** 14206

[24] Medišauskas L, Wragg J, Hart H and Ivanov M Y 2015 *Phys. Rev. Lett.* **115** 153001

[25] Fleischer A, Kfir O, Diskin T, Sidorenko P and Cohen O 2014 *Nat. Photon.* **8** 543

[26] Chen C, Tao Z, Hernández-García C, Matyba P, Carr A, Knut R, Kfir O, Zusin D, Gentry C, Grychtol P, Cohen O, Plaja L, Becker A, Jaron-Becker A, Kapteyn H and Murnane M 2016 *Sci. Adv.* **2** e1501333

[27] Dixit G, Jimeńez-Galań Á, Medišauskas L and Ivanov M 2018 *Phys. Rev. A* **98** 053402

[28] Reich D M and Madsen L B 2016 *Phys. Rev. Lett.* **117** 133902

[29] Long S, Becker W and McIver J K 1995 *Phys. Rev. A* **52** 2262

[30] Eichmann H, Egbert A, Nolte S, Momma C, Wellegehausen B, Becker W, Long S and McIver J K 1995 *Phys. Rev. A* **51** R3414

[31] Kfir O, Grychtol P, Turgut E, Knut R, Zusin D, Popmintchev D, Popmintchev T, Nembach H, Shaw J M, Fleischer A, Kapteyn H, Murnane M and Cohen O 2015 *Nat. Photon.* **9** 99

[32] Zhang H D, Guo J, Shi Y, Du H, Liu H F, Huang X R, Liu X S and Jing J 2017 *Chin. Phys. Lett.* **34** 014206

[33] Pisanty E and Jiménez-Galán Á 2017 *Phys. Rev. A* **96** 063401

[34] Jimeńez-Galań Á, Zhavoronkov N, Schloz M, Morales F and Ivanov M 2017 *Opt. Express* **25** 22880

[35] Milošević D B, Becker W and Kopold R 2000 *Phys. Rev. A* **61** 063403

[36] Pisanty E, Sukiasyan S and Ivanov M 2014 *Phys. Rev. A* **90** 043829

[37] Chen Y J, Fu L B and Liu J 2013 *Phys. Rev. Lett.* **111** 073902

[38] Li W Y, Yu S J, Wang S and Chen Y J 2016 *Phys. Rev. A* **94** 053407

[39] Mauger F, Bandrauk A D and Uzer T 2016 *J. Phys. B* **49** 10LT01

[40] Baykusheva D, Ahsan M S, Lin N and Wörner H J 2016 *Phys. Rev. Lett.* **116** 123001

[41] Liu X, Zhu X, Li L, Li Y, Zhang Q, Lan P and Lu P 2016 *Phys. Rev. A* **94** 033410

[42] Yuan K J and Bandrauk A D 2018 *Phys. Rev. A* **97** 023408

[43] Milošević D B 2015 *Phys. Rev. A* **92** 043827

[44] Zhang X, Li L, Zhu X, Liu X, Zhang Q, Lan P and Lu P 2016 *Phys. Rev. A* **94** 053408

[45] Li P C, Sheu Y L, Laughlin C and Chu S I 2014 *Nat. Commun.* **6** 7178

[46] Heslar J, Telnov D A and Chu S I 2018 *Phys. Rev. A* **97** 043419

[47] Long S, Becker W and McIver J K 1995 *Phys. Rev. A* **52** 2262

[48] Ma X, Zhou Y and Lu P 2016 *Phys. Rev. A* **93** 013425

[49] Wang Z, Li M, Zhou Y, Li Y, Lan P and Lu P 2016 *Phys. Rev. A* **93** 013418

[50] Tong A, Zhou Y and Lu P 2015 *Opt. Express* **23** 15774